

## A DISCUSSION ON MECHANICAL PROPERTIES OF INTERFACE IN REPAIRED CONCRETE BASED ON ANALYSES WITH NEW 2D MODELS

A. SATOH<sup>\*</sup>, K. YAMADA<sup>†</sup> AND S. ISHIYAMA<sup>†</sup>

<sup>\*</sup> Kumamoto University  
2-39-1 Kurokami Kumamoto, 860-8555, Japan  
e-mail: ayumi-s@arch.kumamoto-u.ac.jp, www.murakami-lab.jp/index.html

<sup>†</sup> Akita Prefectural University  
84-4 Aza Ebinokuchi Tsuchiya Yurihonjo City 015-0055, Japan  
e-mail: Kanji\_yamada@akita-pu.ac.jp, Ishiyama@akita-pu.ac.jp,  
www.akita-pu.ac.jp/system/aes/mtrl/archmtl.htm

**Key words:** FEM analysis, concrete, repair, construction joint, adhesion, strength, ductility

**Abstract:** The main theme of this paper is to focus on the mechanisms for achieving high ductility of the interface between substrate concrete and patched repair materials. For that purpose, this paper elaborates the relationship between the mechanical performance of the concrete beam with an interface layer of patched repair and the fractographic characteristics of the fractured surface. The authors conducted four cases of FEM analysis under bending load employing “KAT model”, which the authors newly established. Also experimental investigation was conducted with using the same types of specimens as the FEM analysis. The results from FEM analysis are consistent to the experimental ones in terms of the behavior, mechanical properties and crack paths. The authors conducted the fractographic analysis and found an index which is consistently proportional to the mechanical performance. The simulations by KAT model revealed the mechanisms which lead to high ductility, and it also revealed the mechanisms why the index based on fractographic characteristics has a strong relationship with the mechanical performance.

### 1 INTRODUCTION

Adhesive performance of repaired materials to the substrate concrete is the most important issue for repairing and strengthening of the existing structures. The authors have been studying the issue and one of the fractography-based studies [1] revealed that the crack path near the interface between such materials and substrate concrete would be the meandering one into substrate concrete for achieving high mechanical performance. There should be an analytical study which can reveal the process of the formation of the crack path and discuss the relationship between the mechanical performance and the crack path to offer the clues for the in-depth discussion. For that

purpose, FEM (finite element method) analysis is the best resort.

There are many literatures that studied the modeling and the analytical procedure for FEM. Sadouki [2] presented a new concept called “numerical concrete” with using 2D FEM model which can predict structural performance as well as size effect and crack paths. Tajima [3] analyzed fracture process of plain concrete with using 2D or 3D lattice model. Asai [4] analyzed some RC members also using 2D or 3D lattice model. Nagai [5] analyzed the fracture process of compression member based on 3D particle model where the location and the size of coarse aggregates are copied from the real concrete specimen. These

studies based on the meso-scale model in which coarse aggregates and ITZ (interfacial transition zone) around them are modeled.

In comparison to such large numbers of studies which discuss the monolithic concrete, there are limited numbers of studies [6, 7] which discuss the performance of interface using analytical methods. This paper focuses on discussing the mechanisms for enhancing the performance of the interface with employing FEM analysis, which will have a possibility of contributing to find a new method of enhancing the performance for repairing.

## 2 EXPERIMENT

Mix proportion of concrete for specimens, which is seen in Table 1, is an ordinary mixture of which the water-to-cement ratio is 50%, and compressive strength is 46.3 MPa. The fineness modulus of the aggregate used for the mixture is 4.94.

The authors prepared three types of specimens with varied types of placing joint made from different roughening. Also one type of monolithic specimen was made. Table 2 shows the attributes of specimens. The number of specimens was three for each type, which have a section of 100 mm by 100 mm, and a length of 400mm.

Figure 1 shows the procedure of producing the specimen. After 24 hours from the 1st cast of concrete in the half part of mold, the joint surface was roughened for H494R and H494E. Each of them was roughened with different tool and roughening time, so that they have the different roughness. The specimen H494Rc was roughened at the age of 28 days after the first casting. After the roughening, the concrete was cast in the remained half of mold as depicted in Figure 1. Figure 2 shows the roughened surface of H494E (left) and H494R (right). In the case of H494E, gravels appear on the surface. On the other hand, sand grains appear on the surface of H494R. H494Rc has the same appearance as H494R.

The specimens were cured in water at 20°C for 28 days after the final cast of concrete. A 50mm depth notch was incised at the center of

**Table 1:** Mixproportion of specimens.

W/C (%)	s/a (%)	S/C (%)	Mass per unit volume (kg/m <sup>3</sup> )				
			W	C	S	G	Ad*
50.0	43.0	225	178	356	803	1083	1.78

**Table 2:** Attributes of specimens.

Specimen	Remarks and Surface condition
H494N	Reference with no Joint; Monolithic
H494E	2 <sup>nd</sup> casting after 24hrs from 1 <sup>st</sup> casting Gravels appear on the treated surface
H494R	2 <sup>nd</sup> casting after 24hrs from 1 <sup>st</sup> casting Sand grains appear on the treated surface
H494Rc	2 <sup>nd</sup> casting after 28days from 1 <sup>st</sup> casting Sand grains appear on the treated surface

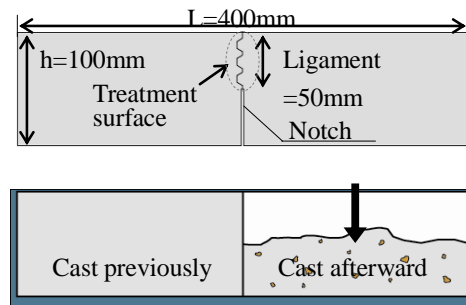


**Figure 1:** Typical detail of specimen (top) and method for producing specimen (bottom).



(a) Surface of H494E (b) Surface of H494R  
**Figure 2:** Appearance of the surface to be jointed.

the specimen before the fracture toughness test. From the test results, mechanical properties and fracture-mechanics-related properties were derived.

## 3 FRACTOGRAPHIC ANALYSIS

After fracture toughness test, fractured surface in the ligament was measured with laser 3-D measuring machine at an interval of 50 $\mu$ m in both x and y directions. Figure 3 depicts the relationship between RL and

mechanical performance. The index RL is a representative index which typifies the crack path. It is a multiplication factor for gaining the real fractured outline length from the projected one.

Figure 4 represents the relationship between RL and mechanical properties. The roughness of H494Rc was slightly smaller than that of H494R, which caused the smaller RL for H494Rc. It is natural that the monolithic specimen has the largest RL and mechanical properties. The important point is that RL and mechanical properties are linearly proportional to the mechanical properties; Fb and  $G_F$ .

It means that the complexity of the fractured surface appears in RL, and RL is deeply related to the adhesion of interface which eventually has the effects on mechanical properties. Mihashi [8] investigated the fractal dimension of the fractured surface of monolithic concrete, and reported that RL is related to the fractal dimension and also mechanical properties. Then it has become clear that RL is also the key index for the mechanical properties of the interface.

## 4 FEM ANALYSIS

### 4.1 KAT Model

The authors developed KAT Model [6] for the FEM simulation and obtained the resulted mechanical properties and crack paths. Figure 5(a) represents the FEM model of a whole bending specimen and Figure 5(b) the part of it with illustrating a detailed composition of KAT model where 6 components (mortar, coarse aggregate, interface, ITZ (interfacial transition zone around aggregate) and mortar\*( mortar near interface)) are depicted.

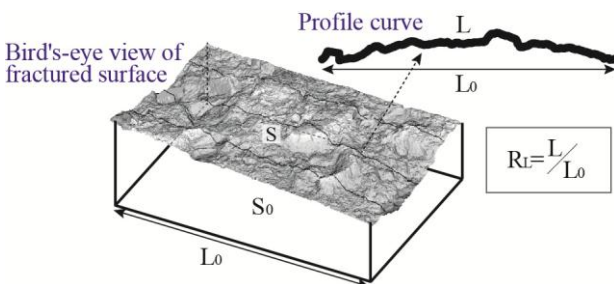
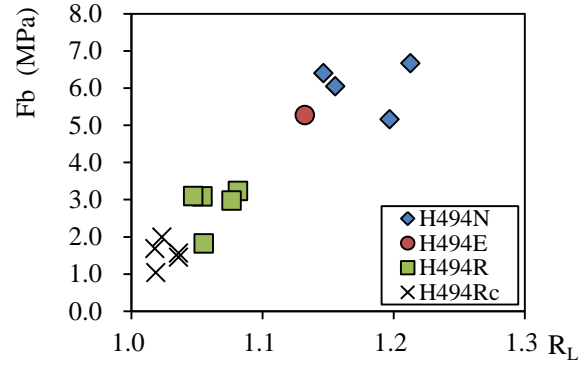
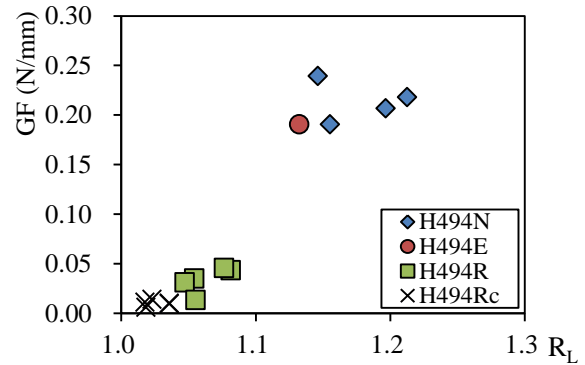


Figure 3: Surface roughness and index RL.

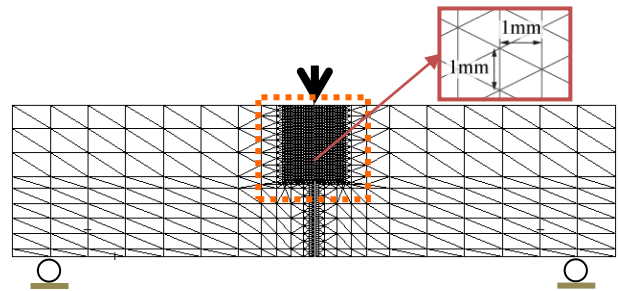


(a) Flexural strength (Fb) vs RL

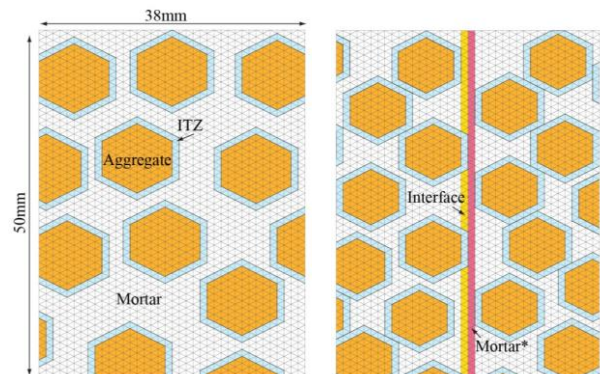


(a) Fracture energy ( $G_F$ ) vs RL

Figure 4: Mechanical properties as a function of RL.



(a) KAT Model for bending member for FEM analysis.



(b) Examples of detailed description of KAT Model depicted in the region enclosed with dotted line in the above : H494N (left) and H494R (right) .

Figure 5: KAT Models.

The main feature of the model is that coarse aggregates are represented by hexagons with only one size which represents the representative size calculated with fineness modulus of the aggregate. The number of them is determined by the unit volume of aggregate in the mixture.

The material properties for FEM were determined by the results from fracture toughness test and from fractured area analysis [7]. Table 3 shows the applied ones.

#### 4.2 Mechanical properties from FEM

Table 4 shows the analyzed and experimental results of mechanical properties. Figure 6(a) and (b) represent the analyzed load-CMOD curves of H494E and H494R respectively, where CMOD is crack mouth opening displacement. Figure 6(c) and (d) represent the crack strain of the elements at the final stage of H494E and H494R respectively, where one can know the final crack path. The final crack path is assumed to be the connected one from the bottom to the top.

Figure 6(a), (b) tells that the predicted responses are consistent to the experimental ones in terms of maximum load and overall behavior including softening behavior which has the ruling effect on ductility.

**Table 3:** Material properties for FEM simulation.

Element	Ft (MPa)	$G_F$ (wof) (N/mm)	Fc (MPa)	E (MPa)
Mortar	7.21	0.060	48	18700
Aggregate	15.00	0.110	80	39000
ITZ	3.90	0.125	30	18700
Interface(R, E)	3.15	0.011	30	18700
Interface(Rc)	2.04	0.005	30	18700
Mortar*	4.00	0.033	30	18700
Concrete	7.50	0.126	48	24000

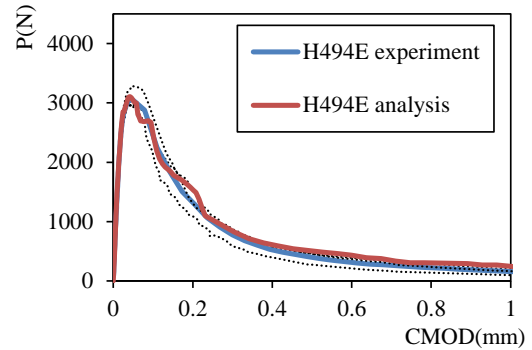
Note: Ft (Tensile strength),  $G_F$  (Fracture energy), Fc (Compressive strength) and E (Elastic modulus). Poisson's ratio is 0.2 for all.

**Table 4:** Analyzed and experimental results.

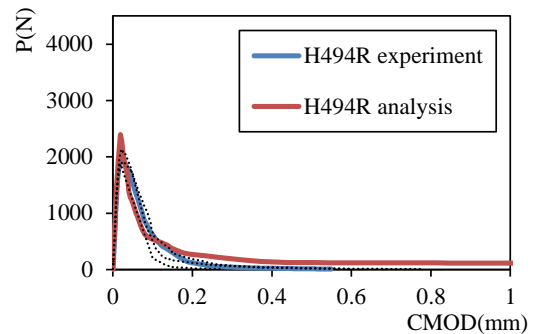
Specimen	Fb (MPa)		$G_F$ (N/mm)	
	Experiment	FEM	Experiment	FEM
H494N	6.75	7.03	0.1336	0.1035
H494E	5.52	5.59	0.1336	0.1355
H494R	3.53	4.31	0.0259	0.0549
H494Rc	1.83	1.86	0.0072	0.0252

The analyzed curve in Figure 6(a) has some dents derived from the easy progress of the crack around ITZ and tough progress of it in mortar. The experimental result does not show such behavior because of the existence of many aggregates at any location of the crack. Figure 6(b) shows the brittle behavior because the crack path is simple progressing along the straight line of the interface and no dents seen in the load-CMOD curve because no aggregate is involved in the crack path.

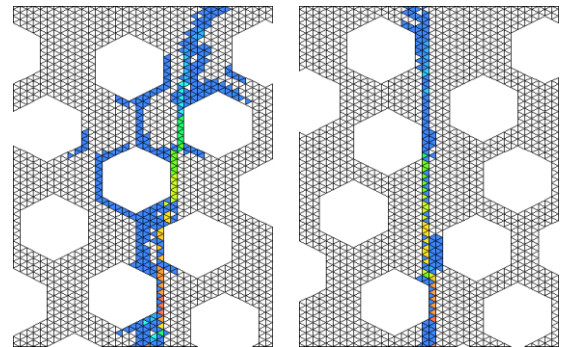
$G_F$  in Table 4 shows the inconsistency of the analyzed one, but it derived from the tendency of holding the load for FEM analysis, which is seen in Figure 6(b).



(a) Load-CMOD curves for H494E.



(b) Load-CMOD curves for H494R.



(c) Crack strain (H494E). (d) Crack strain (H494R).

**Figure 6:** Results from FEM analysis.

### 4.3 RL from FEM analysis

Figure 7 shows the final crack path of H494N achieved from the crack strain. As was described earlier, the final path is the connected one from the bottom to the top. RL is calculated dividing the whole length of the crack path by the projected length.

Figure 8(a) shows the analyzed RL as a function of experimental RL. There is a good agreement between experimental RL and predicted ones, though the analyzed ones are slightly smaller than the experimental ones.

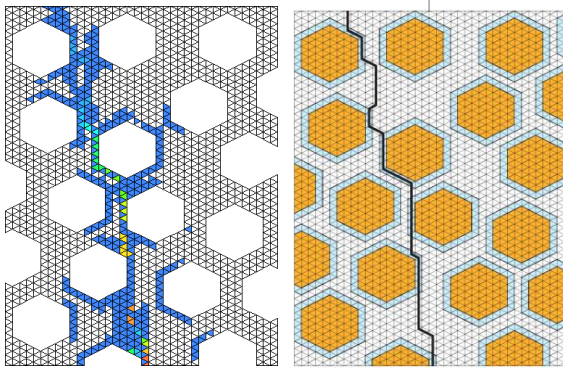
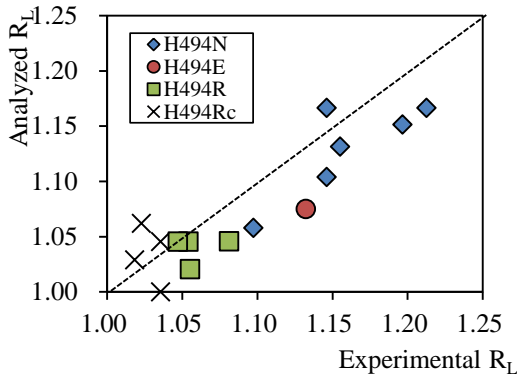
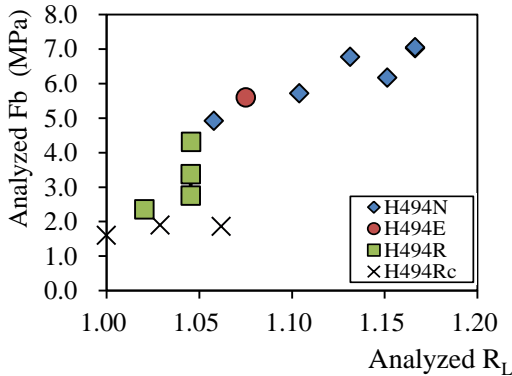


Figure 7: Crack strain (left) and final crack path (right) for H494N.



(a) Analyzed and experimental RL.



(b) Analyzed Fb as a function of analyzed RL.

Figure 8: Analyzed RL.

Figure 8(b) represents the relationship between the analyzed RL and the mechanical properties. One can see that RL has a strong relation to the mechanical properties. As is seen in Figure 4, this tendency is identical to the experimental results.

## 5 ENHANCEMENT OF MECHANICAL PERFORMANCE

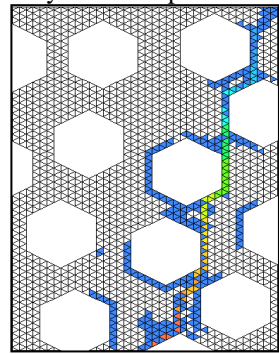
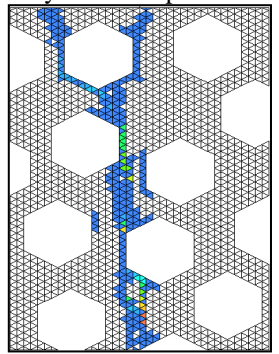
### 5.1 A simulation for improvement of Fb

Table 5 shows the two cases of KAT Model for H494N and the analyzed results. The material properties and the location of aggregates are the same except for the strength of ITZ: Case A has the weak ITZ whereas case B has a strong one.

Different crack paths were produced by the different strengths of ITZ in Table 5. An interesting result is the analyzed Fb: Weak ITZ produced strong Fb whereas the strong ITZ produced weak Fb. This derives from the difference of RL. It means that weak ITZ causes the larger RL than the strong ITZ does, because the crack path tends to proceed in the weakest path along ITZ. But strong ITZ produced the simple straight path, because strength of ITZ is almost the same as the one of mortar where the simple path is the weakest.

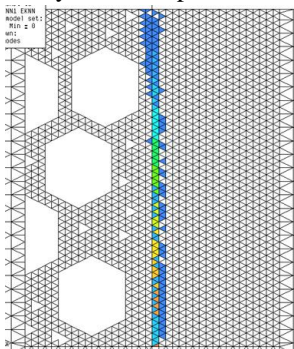
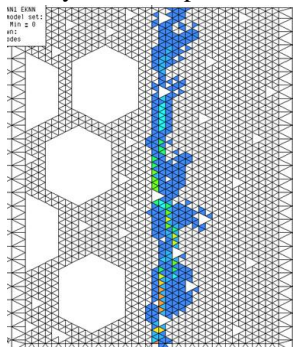
Even though the material strength of the element is weak, large RL can produce large Fb, because Fb is determined by the summed values of multiplied ones by the number of element and the mechanical property of it [6].

Table 5: Two cases of simulation for H494N.

Case A: Weak ITZ Inputted Ft = 3.90 MPa	Case B: Strong ITZ Inputted Ft = 5.66 MPa
Analyzed crack path 	Analyzed crack path 
Analyzed RL = 1.17 Analyzed Fb = 6.75 MPa	Analyzed RL = 1.12 Analyzed Fb = 5.95 MPa

From this result, one new concept for enhancing the mechanical performance can be proposed. It means that the scattering of weak elements moderately in the material would produce the large RL which makes eventually large response. The weak elements to be scattered are ITZ around aggregates, pore and some inclusions. But ordinarily aggregates cannot be scattered deliberately, because they are packed with no room for any other materials in ordinary concrete. So the mortar or repair material can have the possibility of applying for the concept.

**Table 6:** Two cases of simulation for patch repair.

Case CR: No void in PCM	Case CR2: 3% of voids in PCM
Analyzed crack path 	Analyzed crack path 
Analyzed $G_F$ = 0.0403 N/mm Analyzed $F_b$ = 3.86 MPa	Analyzed $G_F$ = 0.192 N/mm Analyzed $F_b$ = 3.58 MPa

Note: PCM is polymer cement mortar for repair.

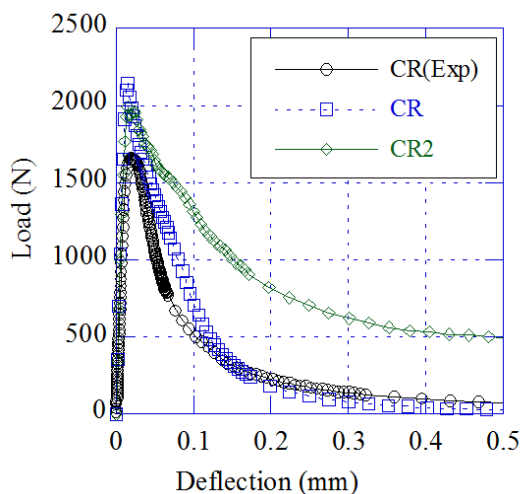


**Figure 9:** Experimental and simulated behaviors.

## 5.2 Effects of diversification of crack path

The authors made another simulation for patch repair. Table 6 represent two cases of simulation for patch repair (right half of the KAT Model) attached to substrate concrete (left half). The detailed material properties and the modeling is described in the reference [7]. The difference between two is only the existence of 3% of voids in the Case CR2, and other material properties and the location of coarse aggregates in substrate concrete is all the same.

Table 6 shows the voids are effective for the diversification of crack path near interface causing a slightly weaker strength but greatly tougher  $G_F$ . About four times of  $G_F$  is achieved from the diversification of crack path in the case of CR2.

Figure 9 represents the load–deflection response of the experimental and two cases of the simulation. The behavior of the simulated CR can be said to be consistent to the one of the experimental results.

## 6 CONCLUSIONS

The experimental investigations and FEM simulations by KAT model revealed the important aspects of enhancing the mechanical properties of the concrete member in bending with an interface layer in it.

One ruling mechanism for leading to the high mechanical performance is expressed in RL which describes the complexity of the crack path being the multiplication factor for gaining the real fractured outline length from the projected one.

The weak interfacial transition zone around the coarse aggregate can make the crack path detour around it eventually producing high strength.

The scattered voids in polymer cement mortar can make the crack path into the repair material generating the diversified crack path in it eventually producing high ductility.

## REFERENCES

- [1] Satoh, A., 2012. A New Concept for Heterogeneity-based Fractography of Concrete. Doctoral dissertation. Akita Pref.

Univ.

- [2] Sadouki, H., Wittmann, F. H., 1995. Numerical Concrete Applied to Investigate Size Effect and Stability of Crack Propagation. In Wittmann F. H. (ed.), *Fract. Mecha. Conc. Str.* 619-634.
- [3] Tajima, K., Shirai, N., 2003. Fracture Analysis of Concrete by 2-Dimensional Particle Model. *J. Struct. Constr. Eng. AIJ.* **571**: 7-14.
- [4] Asai, M., Terada, K., 2003. Meso-Scopic Numerical Analysis of Concrete Structures by a Modified Lattice Model. *J. Struct. Mech. Earthquake Eng., JSCE,* **731**: 43s-54s.
- [5] Nagai, G., Yamada, T., Wada, A., 1998. On a Finite Element Procedure Based on the Real 3-Dimensional Image for Concrete Materials, *J. Struct. Constr. Eng. AIJ,* **509**: 77-82.
- [6] Satoh, A., et. al., 2012. New Box-Counting Method as Interpretation of Crack Paths and Mechanical Properties of Concrete with Interface Layer, In Carpinteri A. (ed.), *Proceedings of Crack Path 2012*, (in print).
- [7] Homma, T., 2012. A Discussion on Fracture Mechanisms and Prediction of Mechanical Properties of Interface in Concrete Employing New Meso-Scale Model, Msc Thesis, Akita Pref. Univ.
- [8] Mihashi, H., Umeoka, T., 1993. Analysis of fractured surface of concrete with aggregates of different size. *J. Struct. Constr. Eng. AIJ.* **453**: 1-7.